Exciton localization by magnetic polarons and alloy fluctuations in the diluted magnetic semiconductor $Cd_{1-x}Mn_xTe$

S. Takeyama, S. Adachi, and Y. Takagi
Faculty of Science, Himeji Institute of Technology, Ako-gun, Hyogo 678-12, Japan

V. F. Aguekian
St. Petersburg University, St. Petersburg 198904, Russia

(Received 1 July 1994; revised manuscript received 14 November 1994)

Photoluminescence was measured on the diluted magnetic semiconductor alloys $Cd_{1-x}Mn_xTe$ with $0.1<x<0.35$, at temperatures between 4.2 and 60 K. Detailed line-shape analysis of the exciton luminescence is carried out to show the temperature dependence of peak positions, integrated intensities, line broadening, and asymmetry of the spectral shape. The luminescence intensity of the so-called L_2 line grows abruptly at low temperatures, and is attributed to exciton localization caused either by exciton magnetic polarons (EMP's) or alloy potential fluctuations (APF's). Only the lowest possible laser-power excitation enables us to observe the effect caused by the former. The characteristic line shape, especially the asymmetry of the luminescence line, is discussed in accordance with a type of localization: EMP's or APF's. We have determined the binding energies of localization from EMP's and APF's, as a function of Mn alloy concentrations. The results are compared with existing theories. It is found that the EMP energy depends on the cube of the number of Mn isolated local spins, and EMP formation is barely realized at $x>0.20$, and most stable at $0.05<x<0.1$. We found that the primary localization due to APF's is not necessary for EMP formation, but that the possibility of spin-fluctuation localization still remains.

I. INTRODUCTION

In the diluted magnetic (or semimagnetic) semiconductors (DMS's) represented by the ternary alloy $Cd_{1-x}Mn_xTe$, local magnetic spins strongly interact with those of electrons or holes in the conduction and the valence band, and therefore cause a variety of substantial spin-related phenomena in optical processes. One of the problems that has recently gained attention is the formation of a free exciton magnetic polaron (EMP), which is associated with a ferromagnetic orientation of magnetic spins within free-exciton Bohr orbits accompanied by a self-trapping localization process.[1,2]

Theoretical estimates of the stability of free magnetic polarons have been presented by Kasuya, Yanase, and Takeda.[3] Various theoretical estimates suggest that the stability conditions for intrinsic EMP's are rarely realized in DMS's, and other primary localization mechanisms are necessary for stable realization of EMP's.[4-6] As distinguished from the bound magnetic polarons (BMP's), EMP's in DMS's are therefore sometimes termed "localized magnetic polarons" as has been pointed out by Mackh *et al.*[7] However, the stability criterion as a function of temperature and concentration of diluted magnetic alloys has been analyzed also by Wolff,[2] who predicted that polaron formation is possible for holes that have large exchange constants and masses. The condition can be satisfied for $\bar{x}>0.05$ at $T=10$ K, where $\bar{x}$ represents the effective concentration of diluted magnetic alloys.

In recent years, studies of time-resolved spectroscopy and/or selective resonant excitations have revealed interesting phenomena originating from EMP's or localized magnetic polarons both in bulk DMS's,[7,9] and in two-dimensional quantum-well systems.[10-12] There have, however, been few systematic experimental surveys on the formation and suppression of EMP's or localized magnetic polarons and their equilibrium stability in external conditions such as temperature and magnetic field.[7,8,13-16] In order to verify the existence of true EMP's, one has to exclude contributions from other localization mechanisms such as spin fluctuations and alloy potential fluctuations (APF's) as has been pointed out by several authors.[7,8] The separation of these effects is in general considered to be difficult, since there are temperature and magnetic-field dependences also of these magnetic and nonmagnetic localization effects. Quite recently, Mackh *et al.* have reported a systematic survey of magnetic polarons evidenced in the exciton photoluminescence (PL) of $Cd_{1-x}Mn_xTe$ by use of selective excitation in the exciton luminescence band and also by picosecond time-resolved spectroscopy.[7] They have discussed the temperature and magnetic-field dependences of the localized magnetic polaron stability and its binding energies with respect to the alloy composition. The existence of intrinsic EMP formation, however, without any help from other sources of localization, has not yet been evidenced experimentally. Accordingly, it can be said that a detailed theory of EMP's has not yet been accomplished. It is our special interest whether the primary localization of excitons such as spin fluctuations and/or APF's is really necessary or not.

The exciton PL spectra possess important information

about the electronic states, exciton scattering, the homogeneity of the sample, impurity centers, and alloy disorder. PL is also very important and useful in studying exciton localization. When the excitation laser power is kept intentionally low, photogenerated excitons in a disordered system relax promptly to the band tail and become localized. These low-energy excitons localize in different parts of a sample and give rise to photoemission with various photon energies due to spatially varying local potentials caused by possible APF's, local spin fluctuations, the magnetic polarons, and other disorder potentials. All these factors yield line broadening and a characteristic spectral shape of the luminescence, especially in the exciton band tail. One should keep in mind that these localized exciton luminescence spectra are in general very sensitive to the excitation laser power, since the number of localization centers is finite. PL studies to probe the exciton localization in semiconductor alloys have been a subject of continuous interest since the work of Cohen and Sturge[17] and other authors. The tail states associated with APF's in semiconductor alloys have been intensively investigated both theoretically[17–19] and experimentally.[17,20] Ouadjaout and Marfaing have categorized and modeled the line shape induced by APF's in accordance with various types of exciton localization: through the electron, through the hole, or by electron-hole confinement.[18]

In the present paper, we present a PL study performed on diluted magnetic semiconductor alloys $Cd_{1-x}Mn_xTe$ with a wide range of manganese concentrations. Detailed line-shape analysis of the luminescence is performed to show the temperature dependence of peak positions, integrated intensities, line broadening, and asymmetry of the spectral shape. We will show that the so-called L_2 PL line at low temperatures is attributed to a localized exciton luminescence caused mainly by EMP's and APF's. An enormous increase of the luminescence intensity at low temperatures is observed, and is attributed to exciton localization due to EMP's. Only the lowest possible laser-power excitation enables us to observe the effect caused by EMP's. The characteristic line shape, especially the asymmetry of the luminescence line, is discussed in accordance with the type of localization based on the model of Ouadjaout and Marfaing: EMP or APF. We have determined the binding energies of localization both from EMP's and APF's as a function of Mn alloy concentrations. The results are compared with existing theories. It is found that the EMP energy depends on the cube of the number of Mn isolated local spins, and EMP formation is barely realized at Mn compositions x higher than 0.20 due to the increased number of antiferromagnetically coupled Mn spin clusters. We insist that primary localization due to APF's is not necessary for EMP formation, but that spin-fluctuation localization may possibly help EMP formation.

II. EXPERIMENT

Samples of $Cd_{1-x}Mn_xTe$ were grown by the modified Bridgman method with nominal Mn mole fraction x values between 0.1 and 0.35. Actual values of x were determined by the peak positions of the L_2 PL line as described in the following section, and the mole fractions of samples used for the measurements were $x=0.10$, 0.12, 0.15, 0.18, 0.20, and 0.35. The samples were selected from those which exhibit more enhanced L_2-(free-exciton-)like lines than L_1-(bound-exciton-)like lines.[1] The samples were either cleaved or polished with bromine-methanol prior to the measurements. A 488-nm Ar-ion laser line was used for the excitation with the lowest possible power less than 1.5 mW/mm^2, and the spot size focused on the sample was about 1 mm^2(<150 mW/cm^2). The very weak PL emission from the sample was detected by an image-intensified charge-coupled device array with a backscattering configuration. The spectral resolution was smaller than 0.1 nm (about 2 meV). All experiments were conducted with the sample mounted in a variable-temperature, exchange-gas Dewar, and the temperature was varied in the range of 4.5–60 K. The sample with $x=0.35$ exhibits its magnetic order as a spin-glass (SG) phase below 9 K, while the others show a paramagnetic phase in the temperature range investigated.[21]

III. RESULTS AND DISCUSSION

A. Temperature variation of L_2 photoluminescence line

Figure 1 demonstrates a typical temperature evolution of the PL lines for $Cd_{1-x}Mn_xTe$ with $x=0.12$. The dominant PL peak is attributed to free-exciton-like recombination (usually labeled L_2), while the small peak at the low-energy side is regarded as the recombination of excitons bound to neutral acceptors (generally labeled L_1 or A^0X).[1] An enormous increase of L_2 luminescence intensity is observed with decreasing temperature apparent-

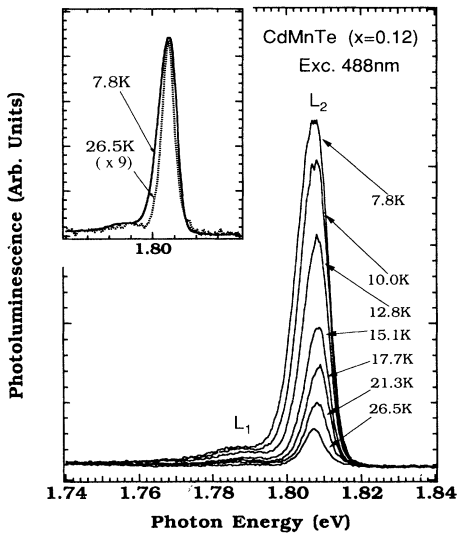

FIG. 1. Typical temperature evolution of the PL lines for $Cd_{1-x}Mn_xTe$ with $x=0.12$. Very weak power of less than 1 mW/mm^2 was used for the excitation with 488-nm Ar-ion laser. The inset displays the comparison of the spectral profile at two different temperatures. Intensity at 26.5 K is multiplied by 9 to normalize the two spectra.

ly below 26 K. Furthermore, as can be seen in the inset where the line at 7.8 K is compared with that at 26.5 K by multiplying the latter to normalize both intensities, it is evident that the PL linewidth at a lower temperature is broader than that at a higher temperature. The linewidth expands more to the low-energy side than to the high-energy side. The spectral line shape is an asymmetrical Gaussian type. This feature is in contrast to the normal case where the linewidth should increase with rising temperature due to the contribution from exciton-phonon interaction. The overall features were the same for all the samples.

In order to clarify the detailed behavior of the L_2 line, the spectra were carefully analyzed. The peak energy and the integrated intensity were determined, and the results are shown in Fig. 2 obtained from the sample with $x=0.18$. As the temperature is decreased, the peak position of the L_2 line first shifts to the high-energy side and then starts to saturate, and finally decreases abruptly below 10 K as displayed in Fig. 2(a). A similar tendency has been demonstrated also by Golnik, Ginter, and Gaj for $Cd_{1-x}Mn_xTe$ samples with x higher than 0.1.[1] The

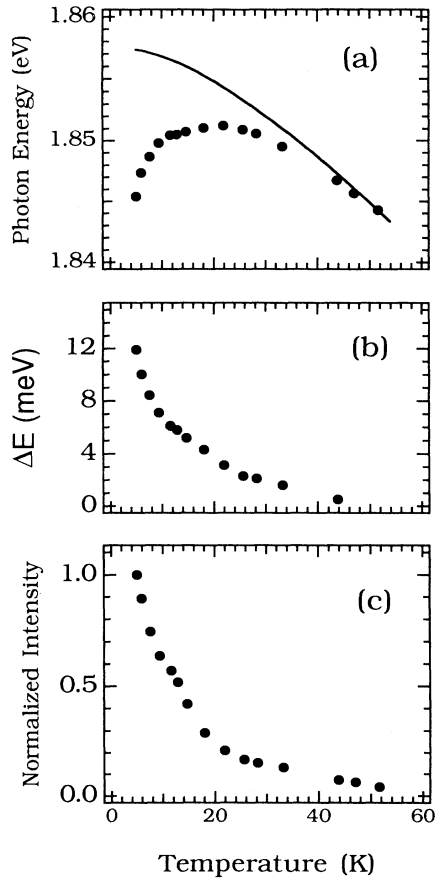

FIG. 2. Temperature variations of (a) the peak positions, (b) energy shift of the peak positions from those expected from high temperatures, and (c) integrated intensity of the L_2 photoluminescence line in Fig. 1. The solid line was obtained from Eq. (1) after adjusting the value x.

temperature dependence of the peak position in the high-temperature region is mainly determined by the dependence of the energy gap on temperature. The shifts of the optical absorption edge with temperature were measured by Sundersheshu and Kendelewicz for $Cd_{1-x}Mn_xTe$ with alloy composition x up to 0.4. They have fitted the data by a formula taking into account the nonlinear dependence,[22] from which the empirical parameters A and B were determined for different Mn compositions. On the other hand, the optical relation for the L_2 peak positions with different Mn compositions were determined by Heiman *et al.* at $T=4$ K.[23] Combining these two relations, one obtains the empirical formula

$$E_{L_2}=\begin{cases} 1.6047+1.397x-\dfrac{AT'^2}{T'+B} & \text{for } 0.05\le x\le 0.2 \\ 1.575+1.536x-\dfrac{AT'^2}{T'+B} & \text{for } 0.2\le x\le 0.4\ , \end{cases} \tag{1}$$

with $T'=T-4$ (K), for the peak position of the L_2 line including temperature dependence.

The solid curve in Fig. 2(a) was obtained as a result of fitting Eq. (1) to the data at higher temperatures than 40 K by varying the x value, where the parameters A and B were taken from the linear interpolation of the data given by Ref. 22. The best optimized value $x=0.181$ agrees well with the nominal one at the initial stage of the crystal growth: $x=0.18$. It is obvious that the experimental data deviate from the solid curve described by Eq. (1) to the low-energy side at temperatures lower than 35 K, and these differences ΔE are plotted in Fig. 2(b). ΔE increases with decreasing temperature, and increases more steeply especially below 10 K. In accordance with this behavior, below 35 K the integrated intensity of the PL line starts to grow gradually, and increases more abruptly below 10 K as seen in Fig. 2(c). The rate of increase with decreasing temperature changes below and above 10 K.

B. Asymmetry of the photoluminescence spectral profile

Figure 3 demonstrates variation of the spectral profile with temperature. The luminescence exhibits changes from Lorentzian above 40 K to Gaussian type below 35 K as displayed in Fig. 3(a). This fact also indicates that the localization of the exciton takes place at temperatures below 35 K for this sample. In the localized temperature region, the luminescence line shows an asymmetric Gaussian line shape. It is to be noticed that the spectra at 21.9 K are more asymmetric than those at 5.0 K. The temperature dependence of the full width at half maximum (FWHM) W and degree of asymmetry A_s is examined and the results are plotted in Figs. 3(b) and 3(c), respectively, where W and A_s are defined as

$$W=H_l+H_h \quad \text{and} \quad A_s=\frac{H_l-H_h}{H_l+H_h}\ . \tag{2}$$

H_h is the energy difference between the peak position and the position of the FWHM on the high-energy side and H_l that on the low-energy side. In Fig. 3(b) $2H_h$ and $2H_l$

are also plotted to show the variation of the asymmetry.

At temperatures higher than 35 K, W increases with increasing temperature mainly due to the contribution from the exciton-phonon interaction, which is generally evidenced in the usual semiconductors. The dotted linear line in Fig. 3(b) was drawn on the basis of Toyozawa's theory in the limit of weak exciton-phonon coupling, which predicts a linear increase of the linewidth at a relatively low temperature.[24,25] Negative values of $A_s \approx -0.1$ at temperatures higher than 40 K also suggest the contribution from the exciton-phonon interaction as discussed in Ref. 25 for the case of the 1s exciton in Cu_2O. The characteristic behavior in this sample is that W increases with decreasing temperature below 35 K, and tends to saturate to the value 10 meV around 10 K. Further decrease of temperature below 10 K results in rapid line broadening. Coincident with the above critical temperatures, the asymmetry A_s increases towards positive values at around 0.1, and then exhibits a tendency to decrease below 10 K.

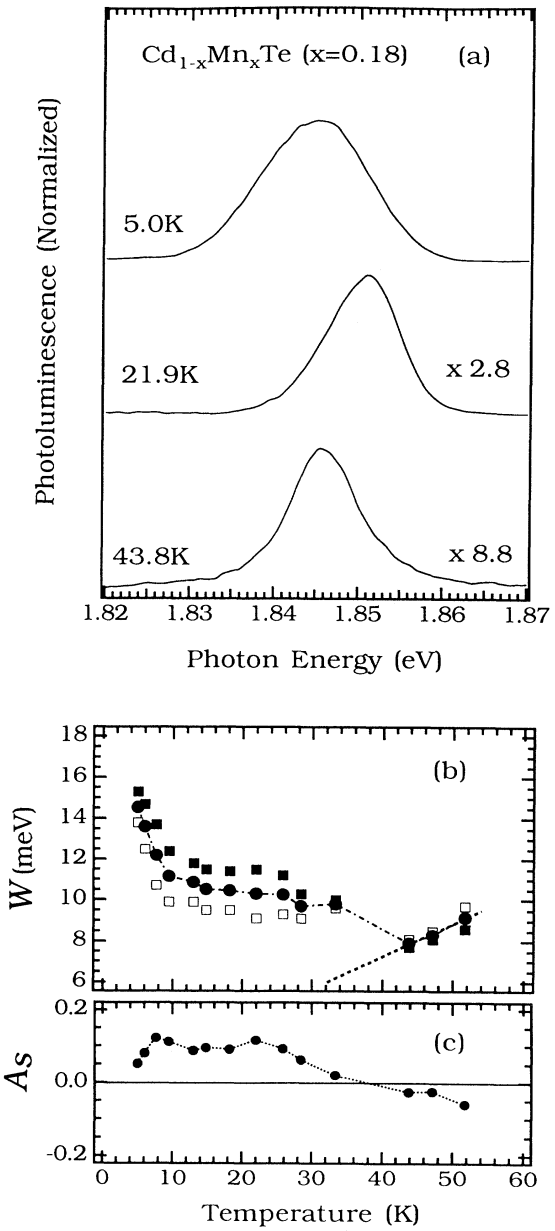

FIG. 3. (a) Typical spectral profiles at three different temperatures. Change of (b) the FWHM (●), $2H_h$ (■), $2H_l$ (□), and (c) asymmetry of the spectra with varying temperatures for $x = 0.18$.

The above features, remarkable energy relaxation, growth of the integrated intensity, and line broadening with variations of asymmetry for the L_2 PL line with decreasing temperatures below 35 K are definitive evidence for exciton localization. This exciton localization regime can be divided into two regions, one at temperatures higher than 10 K and the other at lower than 10 K. As has been discussed by Golnik *et al.*,[1] there are two possible mechanisms responsible for the exciton localization in each temperature regime. One is the usual localization of excitons by APF's, inherent to the mixed crystals due to the band offset between CdTe and MnTe in the present case. The other is a magnetic localization of excitons, which is further separated into two cases. One is the localization by local magnetic spin fluctuations and the other is the exciton localization due to a ferromagnetic orientation of local magnetic spins within the exciton Bohr radius, forming a free EMP.

The degree of asymmetry A_s can be used to judge the type of exciton localization. The exciton PL spectral line shape was theoretically studied and applied to the case of localization due to APF's in II-VI semiconductor compounds by Ouadjaout and Marfaing.[18] According to their simple model with an assumption of a spherical potential well, different kinds of exciton localization are considered, depending on the extension of the potential wells and on the fluctuation amplitude relative to the electon-hole interaction energy: (1) localization of the exciton as a single particle in a localization well, called exciton localization, and (2) localization of one of the exciton components (electron or hole), the other particle being bound by Coulomb interaction, labeled electron (or hole) localization.

The situation for APF's in $Cd_{1-x}Mn_xTe$ is similar to the case of $Hg_{1-x}Cd_xTe$ in the paper by Ouadjaout and Marfaing, and localization of the exciton occurs as a single particle in APF's. In this case the spectral band tail is pronounced and results in increased asymmetry of the spectra with A_s being large. This phenomenon is observed in Fig. 3(c) at temperatures between 35 and 10 K. On the other hand, the magnetic localization of excitons can be considered as a hole localization for the following reason. The exchange interaction with localized Mn spins is four times larger for holes than electrons, and the mass of a heavy hole is about six times larger than that of an electron. A magnetic localization is hence predominantly governed by hole localization. According to Ref. 18, this leads to the increased symmetry of the Gaussian-type spectral line shape and A_s should decrease. This is clearly evidenced below 10 K in Fig. 3(c). Thus measuring A_s is very useful in identifying the type of localization, and is used to separate the EMP localization (hole localization) from that due to APF's (exciton localiza-

tion). The region of temperatures at which either magnetic localization or APF localization dominates as a localization mechanism is judged from the value of A_s.

C. Localization energies of exciton magnetic polarons and alloy potential fluctuations

Based on the above consideration, we attribute the higher-temperature region (10–35 K) to a localization due to APF's, and the low-temperature region (below 10 K) to a magnetic localization of excitons for the sample with $x=0.18$. Both can be considered as the Mott-Anderson picture of localization associated with a mobility edge.[17] The integrated intensity in Fig. 2(c) is replotted against the inverse temperature in order to estimate the thermal binding energy E associated with the localization, assuming that the intensity increase stems from thermally activated localization. The temperature dependence of the PL intensity I is described by a simple formula:

$$I=\frac{I_0}{1+Ce^{-E/k_BT}}, \tag{3}$$

where I_0 and C are constants, and k_B is the Boltzmann constant. Equation (3) is fitted to the data in Fig. 4 at temperature regions I and II, respectively, to obtain the value E. The value $E=1.9$ meV obtained from region I is considered as the thermal binding energy for magnetic localization, while $E=4.1$ meV is determined in region II as the energy for the localization due to APF's.

This type of analysis has been performed for all the other samples with different Mn compositions x. For the sample with x less than 0.12, a type of localization in region I takes place at higher temperatures than type II, i.e., effects of the magnetic localization appear at higher temperatures, and those of APF's influence predominantly at lower temperatures, in contrast to the case for $x\geq 0.18$. The results of the thermal binding energy for each region are displayed in Fig. 5 for different Mn alloy compositions. The E for APF's (open squares) slowly increases with x, and has a tendency to saturate at a value around 8 meV at $x\approx 0.4$. The dotted line in Fig. 5 is plotted on the basis of the model calculation for the localization energy E for APF's by Cohen and Sturge[17] as

$$E\approx\frac{m_h^{ex}}{4\pi\hbar^2 a_B}\left[\frac{dE_g}{dx}\right]^2 x(1-x)\Omega, \tag{4}$$

where Ω is the atomic volume, E_g the band gap, a_B the exciton Bohr radius with the dielectric constant $\varepsilon=9.7$ for CdTe.[26] The heavy-hole exciton mass $m_h^{ex}=m_{HH}+m_e$ and is assumed here as $1.4m_0$. This value is heavier than that for CdTe,

$$m_h^{ex}=0.6m_0+0.096m_0\approx 0.7m_0$$

(Ref. 27). The mass can be heavier as is expected for samples with increased Mn composition. m_h^{ex} for $Cd_{1-x}Mn_xTe$ alloys are, however, not known to our knowledge. The main reason for this big difference stems from the fact that Eq. (4) provides only a qualitative description of the APF energy. The experimentally obtained values E for APF's are thus qualitatively represented by Eq. (4) as shown in Fig. 5. This fact supports the validity of the above analysis to obtain the energy.

Therefore the values E determined as the closed circles in Fig. 5 are regarded as from magnetic localization and monotonically decrease with increasing Mn composition from 8 meV at $x=0.10$ to 0.6 meV at $x=0.20$. This fact is understood as follows. Mn spin clusters favoring antiferromagnetic spin alignment between Mn ions increase with increasing Mn composition, which may compete with the formation of ferromagnetic orientation of the

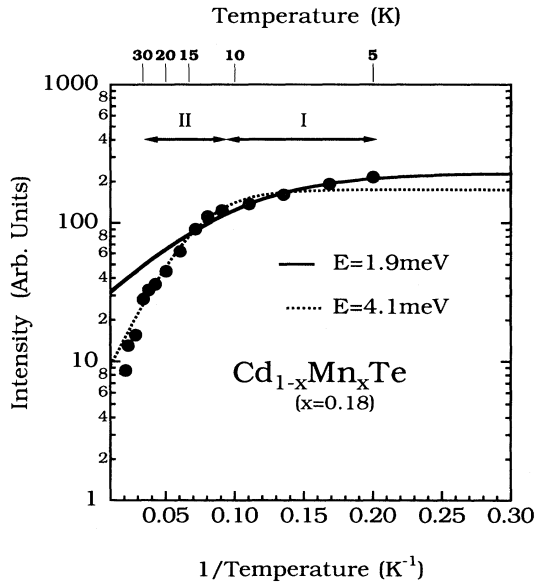

FIG. 4. Integrated intensities of the photoluminescence are plotted against the inverse temperature. The solid and dotted lines are the results obtained by fitting Eq. (3), and activation energies for localization due to EMP's and APF's are determined.

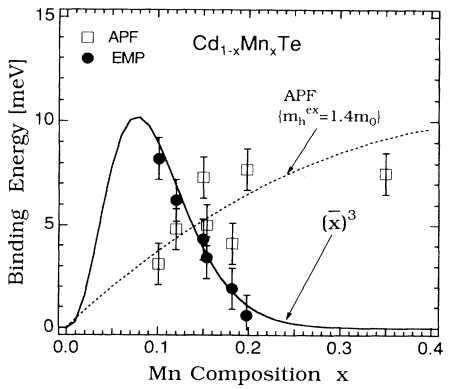

FIG. 5. Binding energies for both EMP's and APF's are determined for different Mn alloy compositions. The dotted line shows the result obtained from Eq. (4), assuming the heavy-hole exciton mass $m_h^{ex}=1.4m_0$. The solid line demonstrates the $(\bar{x})^3$ dependence.

Mn spins in EMP's. Furthermore, at $x \geq 0.20$ a SG phase starts to develop at low temperatures.[28] The SG alignment also contributes to the suppression of EMP formation.[2,16] At present it is assumed that the binding energy thus determined is dominated by an EMP contribution rather than by spin fluctuations. As discussed by Wolff, the stability of the free magnetic polaron is judged from the criterion

$$\frac{(\bar{x})^3(JN_0)^5}{(k_BT)^2(\hbar^2N_0^{2/3}/2m^*)^3} > \pi^2\left[\frac{384}{35}\right]^3, \quad (5)$$

where $\bar{x}$ is the effective Mn^{2+} concentration,

$$\bar{x} = N_0x(1-x)^{12}, \quad (6)$$

J is the exchange constant between carrier spins and Mn local spins, N_0 is the unit-cell density of the crystal, and m^* is the mass of carriers. The above equation is deduced from the analysis by Kasuya, Yanase, and Takeda[3] with the additional condition of spin saturation.[2] The free magnetic polaron must have the requirement of spin saturation in the radius of the carrier wave function. In the present case, EMP's are mainly governed by the hole spin polaron, since the exchange $JN_0 \cong 1$ eV for holes is four times larger than that for electrons, and the hole mass is one order of magnitude greater than that of an electron. At a given temperature T, the polaron stability is proportional to $(\bar{x})^3$, namely, proportional to the cube of the number of isolated local spins as seen in Eq. (5). This $(\bar{x})^3$ dependence is plotted as a solid line in Fig. 5. The present data of EMP's in Fig. 5 agree surprisingly well with the solid line.

According to the estimation by Wolff, taking the values $JN_0 \cong 1.0$ eV and $m^*_{HH} \cong 1m_0$, Eq. (5) gives rise to the polaron stability condition $T < 10$ K for the case of $x = 0.1$ and $T < 4$ K for $x = 0.2$, whereas our data show that the EMP starts to form at $T < 30$ K for $x = 0.1$ and and $T < 10$ K for $x = 0.2$. The critical temperature T_c at which the EMP starts to form varies with Mn compositions, and these data are plotted against Mn mole fractions, together with those deduced from Eq. (5) by a solid line, in Fig. 6. The qualitative dependence agrees very well, but not the absolute value. The difference in the absolute value may come partially from a heavier effective mass than $m^*_{HH} \cong 1m_0$ used in the estimation in this localization regime, where the effective mass is expected to increase with increasing localization. The theory does not take this factor into account. If one assumes the heavier mass as $m^*_{HH} \cong 1.6m_0$ and the more appropriate value of the exchange constant as $JN_0 \cong 1.1$ eV, then one obtains better agreement as shown by the dotted line in Fig. 6.

Another possibility is as follows. In the present investigation we could not succeed in distinguishing the localization effects caused by EMP's from those caused by spin fluctuations. Suppose that the spin fluctuations took place as a primary localization for the EMP as has been pointed in some theories,[4-6] our data overestimate the critical temperature, and result in higher temperatures than those predicted from Eq. (5). The enhanced discrepancy at lower Mn mole fractions implies that the localization by spin fluctuations is more effective at lower Mn concentrations. The present study at least leads to the conclusion that APF is not necessarily a primary localization to trigger EMP formation, as one can see from the data for $x < 0.15$ in Fig. 5. However, direct evidence that the spin fluctuation is or is not responsible for the primary localization for EMP's is still left open for further study.

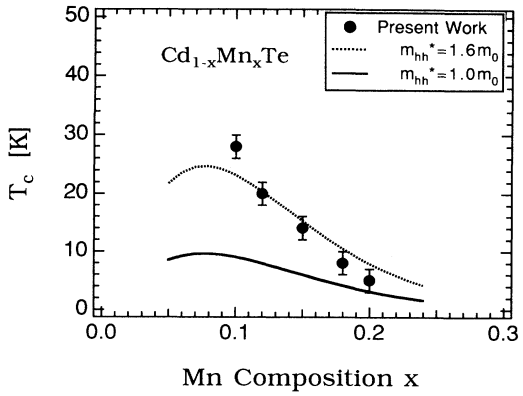

FIG. 6. Variation of the critical temperature T_c at which the EMP starts to form with Mn alloy composition. The solid line represents the values deduced from Eq. (5) with $JN_0 \cong 1.0$ eV and $m^*_{HH} \cong 1m_0$ in accordance with Wolff, and the dotted line with $JN_0 \cong 1.1$ eV and $m^*_{HH} \cong 1.6m_0$.

IV. CONCLUSIONS

A very weak-power excitation PL study on $Cd_{1-x}Mn_xTe$ revealed that both APF's and EMP's contribute to the anomalous evolution of the luminescence intensity at low temperatures. Spectral shape features such as the FWHM, asymmetry, and peak position of the luminescence line also exhibit characteristic features in accordance with the range of temperature at which APF or EMP localization occurs. Thus the effect caused by either APF's or EMP's is separately identified, and the binding energy of each localization was determined as a function of Mn alloy compositions. At Mn compositions $x < 0.15$, the EMP binding energy is larger than that of APF's, but for the sample with high Mn compositions the APF binding energy overcomes the EMP energy. The present data on APF localization energies were compared with theory, and demonstrated a qualitative agreement. While for the EMP energies there is no theory available, our data exhibited an $(\bar{x})^3$ dependence: in other words, the binding energy of EMP's is proportional to the cube of the number of isolated local Mn spins. Increasing antiferromagnetic clusters with increasing Mn composition lead to the decreasing stability of the EMP's, in contrast

to the results recently obtained by Mackh *et al.*[7] Our data concerning the stability of EMP formation, however, qualitatively agree with the theoretical estimation by Wolff for heavy-hole magnetic polarons.[2] Our systematic survey convinces us that APF is not necessarily the primary localization for EMP formation, but the role of spin fluctuations is unknown. The localization effect caused by either APF's or EMP's in external magnetic fields and the excitation laser-power dependencies will be reported in the near future.

ACKNOWLEDGMENTS

This work was partially supported by the Hyogo Science and Technology Association, under Contract No. 6W35, and also by the Saneyoshi Scholarship Foundation. We are also indebted to N. Miura at ISSP and J. Kossut at Institute of Physics, Polish Academy of Sciences for continuous encouragement on this work. Fruitful discussions with D. Heiman at MIT and J. Furdyna at University of Notre Dame are cordially acknowledged.

[1] A. Golnik, J. Ginter, and J. A. Gai, J. Phys. C **16**, 6073 (1983).
[2] P. A. Wolff, in *Diluted Magnetic Semiconductors,* edited by J. K. Furdyna and J. Kossut, Semiconductor and Semimetals Vol. 25 (Academic, London, 1988), p. 413.
[3] T. Kasuya, A. Yanase, and T. Takeda, Solid State Commun. **8**, 1543 (1970).
[4] A. Wolff, D. Heiman, E. D. Esaacs, P. Becla, S. Forner, L. R. Ram-Mohan, D. H. Ridgley, K. Dwight, and A. Wood, in *Proceedings of the International Conference of the Application of High Magnetic Fields in Semiconductor Physics, Würtzburg, 1986,* edited by G. Landwehr (Springer, Heidelberg, 1987), p. 421.
[5] C. Benoit à la Guillaume, Phys. Status Solidi B **175**, 369 (1993).
[6] A. V. Kavokin and K. V. Kavokin, Semicond. Sci. Technol. **8**, 191 (1993).
[7] G. Mackh, W. Ossau, D. R. Yakovlev, A. Waag, G. Landwehr, R. Hellmann, and E. O. Göbel, Phys. Rev. B **49**, 10 248 (1994).
[8] J. J. Zayhowski, C. Jagannath, R. N. Kershow, D. Ridgley, K. Dwight, and A. Wolt, Solid State Commun. **55**, 941 (1985).
[9] Y. Oka, T. Ohnishi, H. Sato, and I. Souma, J. Cryst. Growth **117**, 840 (1992).
[10] D. R. Yakovlev, W. Ossau, G. Landwehr, R. N. Bicknell-Tassius, A. Waag, S. Schmeusser, and I. N. Uraltsev, Solid State Commun. **82**, 29 (1992).
[11] D. R. Yakovlev, J. Phys. (France) IV **3**, C5-67 (1993).
[12] H. Akinaga, K. Takita, S. Sasaki, S. Takeyama, N. Miura, T. Nakayama, F. Minami, and K. Inoue, Phys. Rev. B **46**, 13 136 (1992).
[13] S. Takeyama, S. Adachi, Y. Takagi, N. Miura, and V. F. Aguekian, J. Cryst. Growth **117**, 1081 (1992).
[14] V. F. Aguekian, S. Takeyama, S. Adachi, Y. Takagi, and N. Miura, Solid State Commun. **86**, 205 (1993).
[15] J. J. Zayhowski, R. N. Kershow, D. Ridgley, K. Dwight, A. Wolt, R. R. Galazka, and W. Giriat, Phys. Rev. B **35**, 6950 (1987).
[16] S. Takeyama, S. Adachi, Y. Takagi, and V. F. Aguekian, Jpn. J. Appl. Phys. **32**, Suppl. **32-3**, 425 (1993).
[17] E. Cohen and M. D. Sturge, Phys. Rev. B **25**, 3828 (1982).
[18] D. Ouadjaout and Y. Marfaing, Phys. Rev. B **41**, 12 096 (1990).
[19] S. K. Lyo, Phys. Rev. B **48**, 2152 (1993).
[20] E. D. Jones, R. P. Schneider, Jr., S. M. Lee, and K. K. Bajaj, Phys. Rev. B **46**, 7225 (1992).
[21] R. R. Galazka, S. Nagata, and P. H. Keesom, Phys. Rev. B **22**, 3344 (1980).
[22] B. S. Sundersheshu and T. Kendelewicz, Phys. Status Solidi A **69**, 467 (1982).
[23] D. Heiman, P. Becla, R. Kershaw, D. Ridgley, K. Dwight, A. Wold, and R. R. Galazka, Phys. Rev. B **34**, 3961 (1986).
[24] Y. Toyozawa, Prog. Theor. Phys. **27**, 89 (1962).
[25] T. Itoh and S. Narita, J. Phys. Soc. Jpn. **39**, 140 (1975).
[26] D. Berlincourt, H. Jaffe, and R. L. Shiozawa, Phys. Rev. **129**, 1009 (1963).
[27] *Numerical Data and Functional Relationships in Science and Technology,* edited by O. Madelung, Landolt-Börnstein, New Series, Group III, Vol. 17, Pt. b (Springer, New York, 1982).
[28] S. Oseroff and P. H. Keesom, in *Diluted Magnetic Semiconductors* (Ref. 2), p. 73.